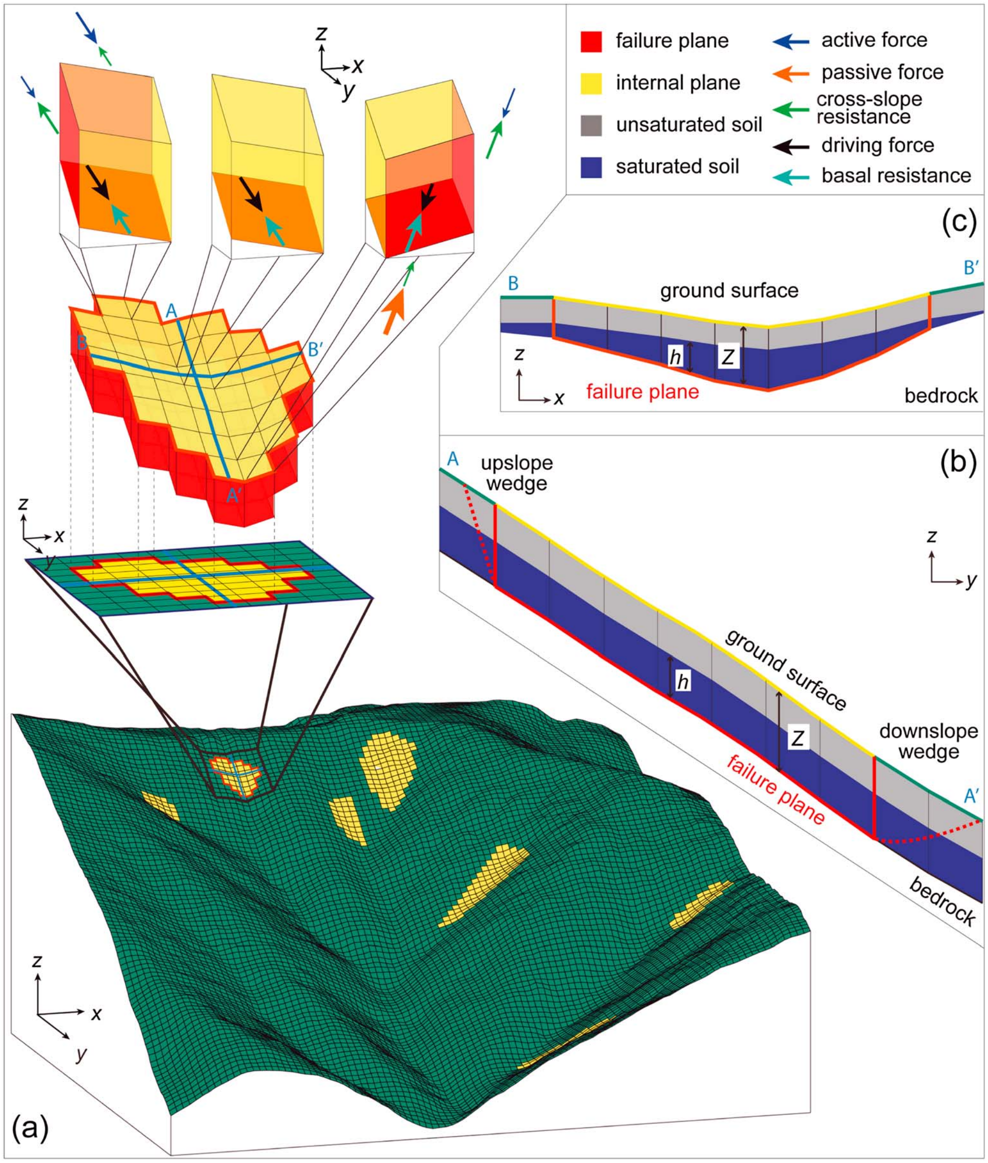

Figure 1. (a) Oblique view of a discretized landscape (Coos Bay, Oregon) showing steep convergent topography with discretized landslides in yellow. The inset shows the CB-1 landslide discretized into columns with landslide margins in red. The collective FS for these columns is the ratio of the total resisting force to the total driving force. Colored arrows show the driving and resistive forces acting on three example columns: an upslope boundary column, an internal column, and a downslope boundary column. Each landslide margin has two forces acting on it because grid cells are not oriented parallel to the slope (see Figure 2b). (b) Profile view of the landslide from A to A′ indicating the upslope and downslope wedges. (c) Cross section from B to B′ where Z is the soil depth and h is the water table height above the failure plane.

The advent of high-resolution topographic data has improved the detection of various types of landslides (e.g., *McKean and Roering* [2004], *Chigira and Yagi* [2006], and review in *Jaboyedoff et al*. [2012]), as well as the application of slope stability models to determine locations with high landslide susceptibility (see reviews in *Casadei et al*. [2003a] and *Simoni et al*. [2008]). However, we currently lack mechanistic models for specifically predicting the location and size of individual shallow landslides across landscapes, thus reducing the effectiveness of landslide hazard delineation and inhibiting our ability to formulate and apply mechanistic models for landslide-derived sediment flux and surface erosion due to landslides [*Dietrich et al*., 2003].

Figure 1 presents an example of a landscape discretized into grid cells, containing information about their physical properties (e.g., elevation, slope, soil depth, contributing drainage area, pore water pressure, and